Dynamic causal modelling of seizure activity in a rat model

*Margarita Papadopoulou[1,2], Gerald Cooray[3, 4], Richard Rosch[3] ,Rosalyn Moran[5], Daniele Marinazzo[1] and Karl Friston[3]

1. Department of Data-analysis, University of Ghent, B9000, Ghent, Belgium
2. INSERM U825, Purpan CHU Hospital, 31059 Toulouse Cedex 3, France
3. The Wellcome Trust Centre for Neuroimaging, University College London, Queen Square, WC1N 3BG, London, UK
4. Clinical Neurophysiology, Karolinska University Hospital, Stockholm, Sweden
5.VTC Research Institute, Bradley Department of Electrical & Computer Engineering, Virginia Tech

Correspondence: Margarita Papadopoulou

Abstract

This paper presents a physiological account of seizure activity and its evolution over time using a rat model of induced epilepsy. We analyse spectral activity recorded in the hippocampi of three rats who received kainic acid injections in the right hippocampus .We use dynamic causal modelling of seizure activity and Bayesian model reduction to identify the key synaptic and activity parameters that underlie seizure onset. Using recent advances in hierarchical modelling (parametric empirical Bayes), we characterise seizure onset in terms of slow fluctuations in synaptic excitability of specific neuronal populations. Our results suggest differences in the pathophysiology of seizure activity in the lesioned versus the non-lesioned hippocampus – with larger changes in inhibition, excitation and temporal summation on the lesioned side.

Introduction

Epilepsy is a common neurological disorder affecting roughly 1% of the population worldwide. Epilepsy is characterised by recurrent and unprovoked seizures, which are caused by abnormal and often hypersynchronous electrical activity in the brain (Blume et al., 2001; Fisher et al., 2005). In order to better understand epileptogenesis, it is necessary to disambiguate among hypotheses concerning the neurophysiological changes that underlie transitions into the seizure state. To address specific mechanistic hypotheses, one can call on animal models of epileptic seizures, and computational formulations of pathological dynamics neuronal networks. Converging evidence from these approaches suggests that seizures are often associated with a persistent excitation-inhibition imbalance (Da Silva et al., 2012); while transitions into seizures can be caused by slow changes in cortical excitability, mediated by modulatory influences on neuronal microcircuitry (Jirsa et al., 2014; Papadopoulou et al., 2015).

Here, we present a model-based analysis of seizure data based on a chemo-convulsant animal model of epilepsy. The use of an animal model allows one to induce seizure activity at a known (hippocampal) location. Intracranial neurophysiological recordings can then be used to estimate the parameters of a neurobiologically plausible model of hippocampal circuitry and thus make empirically informed inferences about changes in excitability and intrinsic connectivity – that cannot themselves be measured directly.

In this paper, we focus on slow changes in cortical excitability, mediated by fluctuations in intrinsic connections. We model the seizure activity induced in rats by kainic acid. We want to establish whether seizure onset is best explained by fluctuations in local dynamics (i.e., intrinsic connectivity), network dynamics (i.e., afferent activity) or both. Furthermore, we try to estimate changes in synaptic efficacy that are necessary to explain the fluctuations in spectral activity that accompany seizure activity. We associate these pathophysiological changes with quantities like extra and intra-cellular electrolytes and neurotransmitters or – in mathematical terms – the slow permittivity variables used in computational models of seizure activity. In subsequent studies, we will use the results of this paper to examine the differences between lesioned and non-lesioned hippocampi – and the evolution of pathophysiology as the seizures develop over a period of weeks.

To characterise the physiological basis of seizure activity, we use biophysically informed modelling with neural mass models and dynamic causal modelling (DCM) (Cooray et al., 2015a; Papadopoulou et al., 2015). Dynamic causal models allow one to predict observed electrophysiological activity (in our case spectral density) in terms of electromagnetic sources that comprise coupled neuronal populations, driven by endogenous neuronal activity (Moran et al., 2009, 2011). These models are equipped with parameters encoding intrinsic connection strengths, synaptic rate constants and the spectral form of endogenous (afferent) input: for a more detailed discussion of the models see (Moran et al., 2013), By epoching electrophysiological data around the point of seizure onset, one can effectively track the trajectory of synaptic parameters that best explains epoch by epoch changes in spectral density during seizure onset. These epoch by epoch changes can be estimated efficiently using hierarchical or parametric empirical Bayesian modelling of DCM parameters (Friston et al., 2015). This paper introduces the application of parametric empirical Bayes to dynamic causal models of seizure onset.

This paper comprises three sections. In the first, we describe the data we analysed and the selection criteria for the three rats studied. This section includes a description of the pre-processing and the computation of spectral density over consecutive epochs of data surrounding seizure onset. The second section provides a brief description of dynamic causal modelling in this context (DCM for cross spectral density), with a special focus on empirical or hierarchical Bayesian modelling that was used to track parameter trajectories. The final section presents the results of Bayesian model comparison for the group of the three rats. We conclude with a discussion of the physiological implications of our results and how these can be used to constrain subsequent studies of the differences between lesioned and non-lesioned hippocampi and the evolution of seizure activity over a period of weeks.

Materials and methods

Data

Wistar rats of approximately the same age and weight were injected with kainic acid (KA) in the right hippocampus. Prior to injection, two depth electrodes were implanted in the right hippocampus of each rat (RH) (dr1 &dr2) separated by 0.5mm; one depth electrode dl was implanted in the left hippocampus (LH) and an epidural electrode was implanted over the right frontal cortex: see Figure 1. A detailed description of the data and surgical procedures can be found in (Raedt et al., 2009). One week after the injection of KA, spontaneous seizures were monitored for a period of 21 weeks. Video-monitoring was performed under environmentally controlled conditions (12 h normal light-dark cycles) in an isolated room.

For this study, we use data recorded from 3 animals (A, B and C). We restrict our analysis to the 10 and 11th week after the injection. This choice was motivated by the fact that all three rats had a consistent number of seizures over that period. The animals are classified in terms of their seizure frequency: Rat B developed more than one seizure per day, while rats A and C had infrequent seizures (less than one per day).

We model the activity of the second depth electrode of the RH (dr2 in Figure 1), and of the single LH electrode (dl in Figure 1). For simplicity, we will refer to these electrodes as RH and LH. For each rat, individual seizures are marked and cross-validated by an expert epileptologist (Readt et al. 2009). The seizure onset was defined visually for each ictal event and confirmed by examining spectral modulations in time-frequency responses around the seizure onset. Peri-ictal segments of approximately 30 seconds are selected and divided into consecutive epochs of 2000ms, overlapping by 800ms. This is the largest epoch size that provided relatively stable frequency responses within each epoch, thus maximising frequency resolution. A Bayesian multivariate autoregressive model was used to estimate the spectral density of the data for each epoch. The resulting spectra were averaged across all peri-ictal epochs for each rat, centred on the seizure onset time. Spectral power between 3-70Hz was modelled. To increase signal-to-noise, spectral activity was smoothed with a Gaussian kernel, with a 2D Gaussian kernel, with a standard deviation of 2.5 and a width of 7 bins in the time domain and 5 bins in the frequency domain

Dynamic causal Modelling

The neural mass model

The peri-ictal activity was modelled using a neural mass model. Four subpopulations are included in the model, two pyramidal cell populations in the pyramidal layer of cornus ammonis 1 and 3 (CA1 and CA3), together with inhibitory interneuron and excitatory cells in the dentate gyrus. This neural mass model has the same structure as the canonical microcircuit model (CMC), used previously in dynamic causal modelling of neocortical activity (Bastos et al., 2012). The CMC model comprises four subpopulations with distinct superficial and deep pyramidal cell populations together with excitatory spiny stellate cells in granular layer IV and inhibitory interneurons in extragranular layers. Although the four neuronal populations all masses were originally motivated for cortical sources, the

modelling of subcortical (e.g., hippocampal) sources with this mixture of inhibitory and excitatory populations appears to provide a sufficient model of hippocampal activity (Moran et al., 2015). Please see Figure 2 for details.

DCM for cross spectral density

The analysis described in this section employs a dynamic causal model of cross spectral densities (CSD) (Moran et al., 2009) – a generalisation of DCM for steady state responses in the complex domain (Friston et al., 2012). In DCM for CSD, neuronal activity is summarised in terms of its spectral density (when modelling a single source) or cross spectral density (when modelling multiple sources).

In this work, we model each (right and left hippocampal) source separately for all three rats. In other words, our focus was on changes in intrinsic connectivity among the four populations within each source, where afferent input from other sources was modelled in terms of endogenous (scale free) fluctuations. These afferent inputs entered at the dental gyrus granular layer (Figure 2). In brief, this allowed us to parameterise spectral activity in each source, in terms of intrinsic connectivity within and between each subpopulation – and the amplitude and (scaling) exponent of endogenous activity. After estimating these parameters for each 2000 ms epoch, we were then able to test models in which one or more of these biophysical parameters changed during the course of seizure onset, using hierarchical or empirical Bayesian modelling. See Table 1 for a list of the parameters that were estimated for each epoch.

Tracking changes in intrinsic connectivity and endogenous activity over time

The free parameters quantifying (intrinsic) connectivity and synaptic constants were estimated using standard Bayesian model inversion procedures. We considered 24 parameters (see Table 1 for more details) that were estimated for each epoch in each rat, allowing the parameters to change over successive epochs. This within-epoch inversion used the usual variational Bayesian scheme under the Laplace approximation (i.e., Variational Laplace).

This model inversion provides posterior expectations and covariances over the free parameters for each epoch. These (first level or within epoch) estimates are then used to model between-epoch effects, using hierarchical or empirical Bayes, described in detail in (Litvak et al., 2015) and (Friston et al., 2015). In brief, this analysis allows for random effects at the between-epoch level that are supplemented by systematic changes over epochs. These changes were modelled using a (between-epoch) general linear model (GLM). Here, the general linear model comprised a temporal basis set, modelling abrupt changes at seizure onset and subsequent decay. One can then use Bayesian model comparison to compare different general linear models of DCM parameter trajectories over epochs. In particular, one can use Bayesian model reduction to eliminate redundant second level (GLM) parameters encoding parameter trajectories.

More specifically by using Bayesian model comparison in this framework, we are able to compare different (second level or between epoch) general linear models that allow for different combinations of connectivity (and endogenous activity) parameters to change over time. These changes are parameterised in terms of the second level parameters that scale the contribution of tonic (sustained) changes at seizure onset and subsequent transient changes, for each first level connectivity parameter. Bayesian model comparison therefore enabled us to identify which DCM parameters are needed to explain changes in cross spectral density during seizure onset – and whether these changes are sustained or transient. Our Bayesian model comparison rests on Bayesian model reduction, which provides an efficient way to compare reduced versions of a full model (where all possible parameters can change) in terms of model evidence (Friston et al., 2015).

Given that endogenous input can change over time, our first question is which changes in intrinsic connectivity (first 14 parameters of Table 1) are necessary to explain observed seizure activity. We then ask a complementary question: given that intrinsic connectivity can change, which changes in endogenous activity are necessary to explain seizure activity (last 10 parameters of Table 1). In summary, we used Bayesian model reduction to compare all possible combinations of changes in intrinsic connectivity parameters, while treating endogenous activity parameters as fixed effects. We then repeated the Bayesian model reduction, comparing all combinations of endogenous activity parameters, while treating connectivity parameters as fixed effects. The results of this Bayesian model reduction or comparison are summarised in terms of Bayesian model averages over second level GLM parameters encoding trajectories or changes in first level DCM parameters.

All the routines used in this analysis are available as part of the academic SPM software: http://www.fil.ion.ucl.ac.uk/spm.

Results

Seizure activity

Figure 3 shows the average activity recorded around three seizures, for both RH and LH sources of one rat in time and frequency. These responses show a synchronous onset of increased power across frequency bands at seizure onset. Figure 4 provides an example of a single seizure.

First level (within epoch) DCM inversion

Figure 5 shows the time-frequency representation of smoothed spectral activity for each rat and the predicted responses following inversion of the DCM (for both hippocampal sources). The similarity between the observed and predictive responses reflects the accuracy of the DCM in explaining fluctuations in spectral density. Crucially, because we have an explicit forward model of these responses, we can also estimate the time frequency activity in each of the populations comprising each source. These are shown in Figures 6 and 7 that show the diversity of spectral responses. Systematic changes that are conserved over seizures appear to be an expression of fast activity following seizure onset in the excitatory cells receiving endogenous input (these are shown in the upper left panels). This is accompanied by increases in power at lower (beta) frequencies in the superficial pyramidal populations (excitatory output cells), with less marked changes in the alpha

range in deep pyramidal cells. The key question now is how are these changes mediated in terms of the underlying synaptic efficacy of intrinsic connections?

For the second level analysis we pooled the data for each hippocampal source over the 3 rats: the second level (GLM) design matrix is shown in Figure 8. Using Bayesian model reduction we tested for all combinations of (sustained and transient) changes in DCM parameters that are necessary to explain seizure activity. We repeat the procedure for the lesioned (RH) and the non-lesioned (LH) hippocampi.

Lesioned hippocampus (see Figure 9): for the effect of onset (tonic changes) described by the first covariate we found that two parameters show marked decreases at seizure onset; namely the T4 and G4 parameters of Table 1. These two parameters encode the synaptic time constant of the pyramidal cells in CA1 (T4), and the self-inhibition of inhibitory interneurons in the pyramidal strata (G4). The latter effect is particularly interesting because it suggests that seizure activity is associated with a disinhibition of inhibitory interneurons. This may sound counterintuitive; however, fast synchronous activity (of the sort associated with desynchronization and cortical excitability) is thought to depend on inhibitory interneurons, and their interactions with pyramidal cells (Isaacson and Scanziani, 2011). For the monotonic decay which is described by the second (monotonic decay) temporal basis function, the same parameters, T4 and G4 parameters show a marked effect.

In the non-lesioned hippocampus (see Figure 10) the tonic changes were explained by two connectivity parameters, encoding the self-inhibition of inhibitory interneurons (G4) and the intrinsic excitatory connections from interneurons in the dental gyrus to pyramidal cells in CA3 (G8). Moreover, there was a monotonic decay in the same two parameters as seen above, together with the synaptic rate constant of interneurons of the dentate gyrus (T1).

Finally, we asked which changes in endogenous activity are necessary to explain seizure activity. For the lesioned hippocampus, the results are shown in Figure 11 for both temporal basis functions. For the tonic or sustained changes the results suggest that changes in all endogenous activity parameters were necessary; however, the most marked effect is carried by the second parameter, controlling the exponent of scale-free endogenous activity. For the second temporal basis function, the number of endogenous parameters needed to explain seizure activity is reduced to the first two endogenous constants of Table 1 (a1 and a2). For the non-lesioned hippocampus (see Figure 12) almost all the parameters of endogenous activity were necessary to explain seizure activity and for the second temporal basis function, we only found changes in the endogenous input, d5 and d7 of Table 1.

Discussion

We have introduced a novel approach to the Bayesian inversion of hierarchical models of laminar-specific neuronal population responses based on neurophysiological recordings. Using biophysically plausible models of neuronal activity enables one to make inferences about hidden neuronal states – and the microcircuitry mediating their dynamics – that are not themselves directly measurable.

This allows one to test specific hypotheses about the pathophysiology underlying an observed neurophysiological measurement.

Here, we used the dynamic causal modelling framework to model hippocampal seizures recorded invasively in a chemoconvulsant-induced animal model of focal epilepsy. By explicitly modelling changes in synaptic activity and afferent input over time, we could then use the empirical measurements to identify the key changes in microcircuitry producing seizure onset: having estimated the neuronal parameters underlying the spectral density of activity in short epochs around seizure onset, we used parametric empirical Bayesian modelling to estimate the parameter trajectories over successive epochs. This involved specifying a hierarchical model of first level (within epoch) spectral activity and a second level of (between epoch) fluctuations in the parameters of the first level.

Intrinsic connectivity changes in the lesioned hippocampus

Initial fitting of a full DCM to empirical data allows all the parameters of the neural mass model to change (within the complexity constraints implicit in the estimation), in order to explain the data features observed in each epoch. Using parametric empirical one can then finesse the inference by testing hypotheses about between epoch changes. In this paper, we applied (parametric) empirical Bayesian (PEB) modelling to identify which DCM parameters are necessary to explain spectral activity during seizure onset.

A relatively small number of synaptic parameters are sufficient to explain the seizure onset in the lesioned hippocampus. These entail either increases in excitation (DG to CA3, CA1 to pyramidal inhibitory cells), disinhibition (self-inhibition of inhibitory cells), and synaptic rate constant decreases (CA1 pyramidal cell). Given the microcircuitry of self-inhibitory and coupled excitatory-inhibitory populations, these results speak to the existing literature on seizure initiation in the context of an excitation-inhibition imbalance. Interestingly, reductions in synaptic pyramidal rate constants further add to this picture, with an increasing window for the synaptic integration of presynaptic input; i.e., the slower post-synaptic decay of signals in CA1 pyramidal neurons. In other words, pre-synaptic inputs are allowed to accumulate, enabling temporal summation of presynaptic inputs (Koch et al., 1996). As CA1 pyramidal cells are one of the main output cell populations in the model, this change in temporal summation – as estimated by fluctuations in synaptic time constants – may indicate an important mechanism for promoting synchronised activity and subsequently enabling seizure spread.

Intrinsic connectivity changes in the non-lesioned hippocampus

As with the directly lesioned hippocampus, there was a small subset of neuronal parameters, whose fluctuations were sufficient to explain the seizure onset. There were two dominant effects; namely, the increase in self-inhibition of inhibitory interneurons (producing an overall disinhibition), and a smaller reduction in excitation in faster neuronal populations (DG CA3), which appears coincident with a small, transient reduction in the DG synaptic rate constant.

Interestingly, the increases in excitation and changes in CA1 synaptic rate constants that were necessary in the lesioned hippocampus to explain spectral responses, are absent in the non-lesioned hippocampus. This suggests that, mechanistically, the evolving seizure on the non-lesioned side is due to synaptic changes that are distinct from changes on the lesioned side – a finding consistent with the fact that observed seizures in the non-lesioned side are probably due to seizure spread, rather than activity in a seizure onset zone. The disinhibition account of seizure recruitment is consistent with the *in vivo* and *in vitro* literature that suggests an initial inhibitory constraint limiting seizure spread, with seizures only promulgating after the constraint is overcome – and the local microcircuitry can be recruited in full (Trevelyan and Schevon, 2013).

Endogenous activity contributions to seizure

Seizure initiation requires changes in all parameters describing the endogenous input to the dentate gyrus on both the lesioned and non-lesioned sites. This would indicate the importance of other cortical circuits with afferent connections to the hippocampus in seizure initiation. The inference made in this study does not allow for any further specification of this activity. Afferent and efferent projections to the hippocampus come partly from contralateral hippocampus and through the six layered entorhinal cortex. Our results speak to the importance of contralateral hippocampal connections for seizure initiation and reciprocal connectivity with the entorhinal cortex. However, it is interesting that the endogenous input differed between lesioned and non-lesioned hippocampus, which suggests that both hippocampi are involved in a network with asymmetrical connections as could be expected. The parameters involved in modulations of endogenous activity – during seizure onset – suggest a more synchronised pattern, with a preponderance of lower frequencies, relative to high frequencies. Anecdotally, this fits with the increase in lower frequencies expressed in the pyramidal populations during seizure activity.

Modelling seizure mechanisms

Our modelling assumed an adiabatic approximation of the generative model, allowing for a hierarchical two level model. The fast states of the first level were assumed to reach steady state within each inverted window, which allows for a simplification – as the spectrum of the data within each epoch could be inverted separately. We then used temporal basis functions, modelling slow dynamics, to model parameter trajectories with a second level model. The implicit simplifications ensure the numerics of the inversion are tractable. Similar analyses has been reported previously in the setting of epilepsy and DCM (Cooray et al., 2015b; Papadopoulou et al., 2015). Furthermore, the above (adiabatic) assumptions have some biological support – as several studies have shown the presence of slowly varying parameters during seizure activity (Kager et al., 2000; Ullah et al., 2009; Wei et al., 2014).

Conclusions

We used Dynamical Causal Model to model peri-ictal brain activity recorded in both hippocampi of rats whose right hippocampus had been injected with kainic acid. We characterised the pathophysiology of seizure onset in terms of physiologically plausible variables such as changes in synaptic efficacy and rate constants. We presented a worked example of empirical Bayesian analyses of seizure activity during seizure onset, which was able to identify the synaptic parameters implicated in epileptogenesis. These parameters might be useful as biomarkers of different types of seizures and their frequency, both in humans and in animal models.

Acknowledgments

KJF is funded by a Wellcome Trust Principal Research Fellowship (Ref: 088130/Z/09/Z).

Software note: the analyses reported in this paper can be reproduced using the academic freeware available from: http://www.fil.ion.ucl.ac.uk/spm/. Dynamic causal modelling of cross spectral density can be implemented using the DCM Toolbox.

References

Bastos AM, Usrey WM, Adams RA, Mangun GR, Fries P, Friston KJ (2012) Canonical microcircuits for predictive coding. Neuron 76:695–711.

Blume WT, Lüders HO, Mizrahi E, Tassinari C, van Emde Boas W, Engel J (2001) Glossary of descriptive terminology for ictal semiology: report of the ILAE task force on classification and terminology. Epilepsia 42:1212–1218.

Cooray GK, Sengupta B, Douglas P, Englund M, Wickstrom R, Friston K (2015a) Characterising seizures in anti-NMDA-receptor encephalitis with Dynamic Causal Modelling. Neuroimage.

Cooray GK, Sengupta B, Douglas P, Friston K (2015b) Dynamic Causal Modelling of Electrographic Seizure Activity using Bayesian Belief Updating. Neuroimage 125:1142–1154.

Da Silva FHL, Gorter JA, Wadman WJ (2012) Epilepsy as a dynamic disease of neuronal networks. Handb Clin Neurol 107:35–62.

Fisher RS, van Emde Boas W, Blume W, Elger C, Genton P, Lee P, Engel J (2005) Epileptic seizures and epilepsy: definitions proposed by the International League Against Epilepsy (ILAE) and the International Bureau for Epilepsy (IBE). Epilepsia 46:470–472.

Friston KJ, Bastos A, Litvak V, Stephan KE, Fries P, Moran RJ (2012) DCM for complex-valued data: cross-spectra, coherence and phase-delays. Neuroimage 59:439–455.

Friston KJ, Litvak V, Oswal A, Razi A, Stephan KE, van Wijk BCM, Ziegler G, Zeidman P (2015) Bayesian model reduction and empirical Bayes for group (DCM) studies. Neuroimage.

Isaacson JS, Scanziani M (2011) How inhibition shapes cortical activity. Neuron 72:231–243.

Jirsa VK, Stacey WC, Quilichini PP, Ivanov AI, Bernard C (2014) On the nature of seizure dynamics. Brain 137:2210–2230.

Kager H, Wadman WJ, Somjen GG (2000) Simulated seizures and spreading depression in a neuron model incorporating interstitial space and ion concentrations. J Neurophysiol 84:495–512.

Koch C, Rapp M, Segev I (1996) A Brief History of Time (Constants). Cereb Cortex 6:93–101.

Litvak V, Garrido M, Zeidman P, Friston K (2015) Empirical Bayes for Group (DCM) Studies: A Reproducibility Study. Front Hum Neurosci 9:670.

Moran R, Pinotsis DA, Friston K (2013) Neural masses and fields in dynamic causal modeling. Front Comput Neurosci 7:57.

Moran RJ, Jones MW, Blockeel AJ, Adams RA, Stephan KE, Friston KJ (2015) Losing control under ketamine: suppressed cortico-hippocampal drive following acute ketamine in rats. Neuropsychopharmacology 40:268–277.

Moran RJ, Jung F, Kumagai T, Endepols H, Graf R, Dolan RJ, Friston KJ, Stephan KE, Tittgemeyer M (2011) Dynamic causal models and physiological inference: a validation study using isoflurane anaesthesia in rodents. PLoS One 6:e22790.

Moran RJ, Stephan KE, Seidenbecher T, Pape H-C, Dolan RJ, Friston KJ (2009) Dynamic causal models of steady-state responses. Neuroimage 44:796–811.

Papadopoulou M, Leite M, van Mierlo P, Vonck K, Lemieux L, Friston K, Marinazzo D (2015) Tracking slow modulations in synaptic gain using dynamic causal modelling: validation in epilepsy. Neuroimage 107:117–126.

Raedt R, Van Dycke A, Van Melkebeke D, De Smedt T, Claeys P, Wyckhuys T, Vonck K, Wadman W, Boon P (2009) Seizures in the intrahippocampal kainic acid epilepsy model: characterization using long-term video-EEG monitoring in the rat. Acta Neurol Scand 119:293–303.

Trevelyan AJ, Schevon CA (2013) How inhibition influences seizure propagation. Neuropharmacology 69:45–54.

Ullah G, Cressman JR, Barreto E, Schiff SJ (2009) The influence of sodium and potassium dynamics on excitability, seizures, and the stability of persistent states. II. Network and glial dynamics. J Comput Neurosci 26:171–183.

Wei Y, Ullah G, Schiff SJ (2014) Unification of neuronal spikes, seizures, and spreading depression. J Neurosci 34:11733–11743.

Table 1

parameter	Type of connection	Origin	Target
T1	synaptic constant	ss	N/A
T2	synaptic constant	sp	N/A
T3	synaptic constant	ii	N/A
T4	synaptic constant	dp	N/A
G1	intrinsic inhibitory	ss	ss
G2	intrinsic inhibitory	sp	ss
G3	intrinsic inhibitory	ii	ss
G4	intrinsic inhibitory	ii	ii
G5	intrinsic excitatory	ss	ii
G6	intrinsic excitatory	dp	ii
G7	intrinsic inhibitory	sp	sp
G8	intrinsic excitatory	ss	sp
G9	intrinsic inhibitory	ii	dp
G10	intrinsic inhibitory	dp	dp
a1	endogenous input spectral amplitude		ss
a2	endogenous input spectral decay over frequency		ss
d1	endogenous input spectral innovation		ss
d2	endogenous input spectral innovation		ss
d3	endogenous input spectral innovation		ss
d4	endogenous input spectral innovation		ss
d5	endogenous input spectral innovation		ss
d6	endogenous input spectral innovation		ss
d7	endogenous input spectral innovation		ss
d8	endogenous input spectral innovation		ss

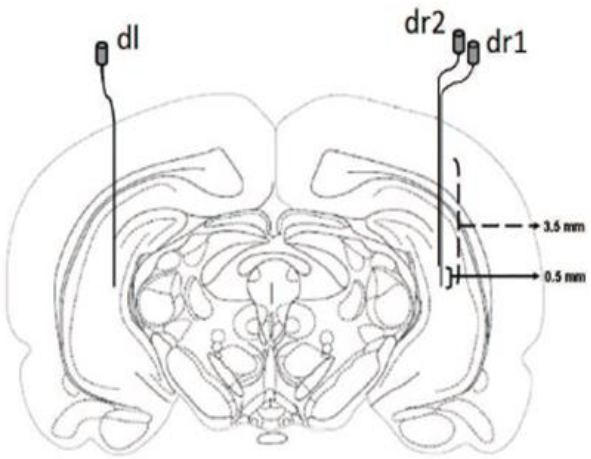

Figure 1. Illustration of the position of the hippocampal depth electrodes. All rats were implanted with two depth electrodes in the RH (**dr1** & **dr2**) and one in the LH (**dl**).

$$\dot{x}_3 = x_4$$
$$\dot{x}_4 = \kappa_e H_e g_8 \sigma(x_1) - \kappa_e H_e g_7 \sigma(x_3) - 2\kappa_e x_4 - \kappa_e^2 x_3 + I$$

$$\dot{x}_5 = x_6$$
$$\dot{x}_6 = \kappa_e H_e g_5 \sigma(x_1) - \kappa_e H_e g_6 \sigma(x_7) - 2\kappa_e x_6 - \kappa_e^2 x_5 + I$$

$$\dot{x}_1 = x_2$$
$$\dot{x}_2 = \kappa_e H_e g_3 \sigma(x_5) - \kappa_e H_e g_1 \sigma(x_1) - 2\kappa_e x_1 - \kappa_e^2 x_2 + I$$

$$\dot{x}_7 = x_8$$
$$\dot{x}_8 = \kappa_e H_e g_{10} \sigma(x_7) - \kappa_e H_e g_9 \sigma(x_5) - 2\kappa_e x_8 - \kappa_e^2 x_7 + I$$

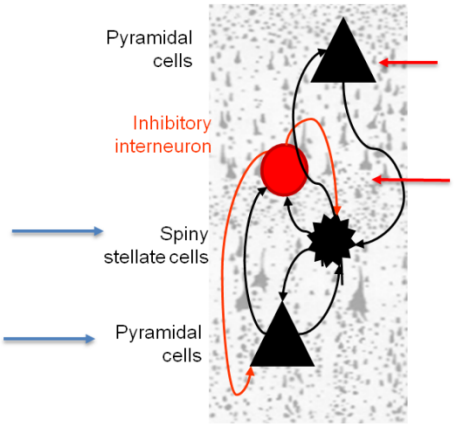

free parameters on time constants and intrinsic connections

G(:,1) ss -> ss (-ve self)
% G(:,2) sp -> ss (-ve rec)
G(:,3) ii -> ss (-ve rec)
G(:,4) ii -> ii (-ve self)
G(:,5) ss -> ii (+ve rec)
G(:,6) dp -> ii (+ve rec)
G(:,7) sp -> sp (-ve self)
G(:,8) ss -> sp (+ve rec)
G(:,9) ii -> dp (-ve rec)
G(:,10) dp -> dp (-ve self)

Neuronal states (deviations from baseline firing)

S(:,1) - voltage (spiny stellate cells)
S(:,2) - conductance (spiny stellate cells)
S(:,3) - voltage (superficial pyramidal cells)
S(:,4) - conductance (superficial pyramidal cells)
S(:,5) - current (inhibitory interneurons)
S(:,6) - conductance (inhibitory interneurons)
S(:,7) - voltage (deep pyramidal cells)
S(:,8) - conductance (deep pyramidal cells)

Extrinsic Connections:
forward (i) sp -> ss (+ve)
forward (ii) sp -> dp (+ve)
backward (i) dp -> sp (-ve)
backward (ii) dp -> ii (-ve)

Figure 2 illustration of the CMC model. This provides the differential equations describing the neuron mass model, with four subpopulations, each described with two differential equations. The left hand panel provides the mathematical form of the model, while the right-hand panel shows how we assign these populations to the hippocampal populations.

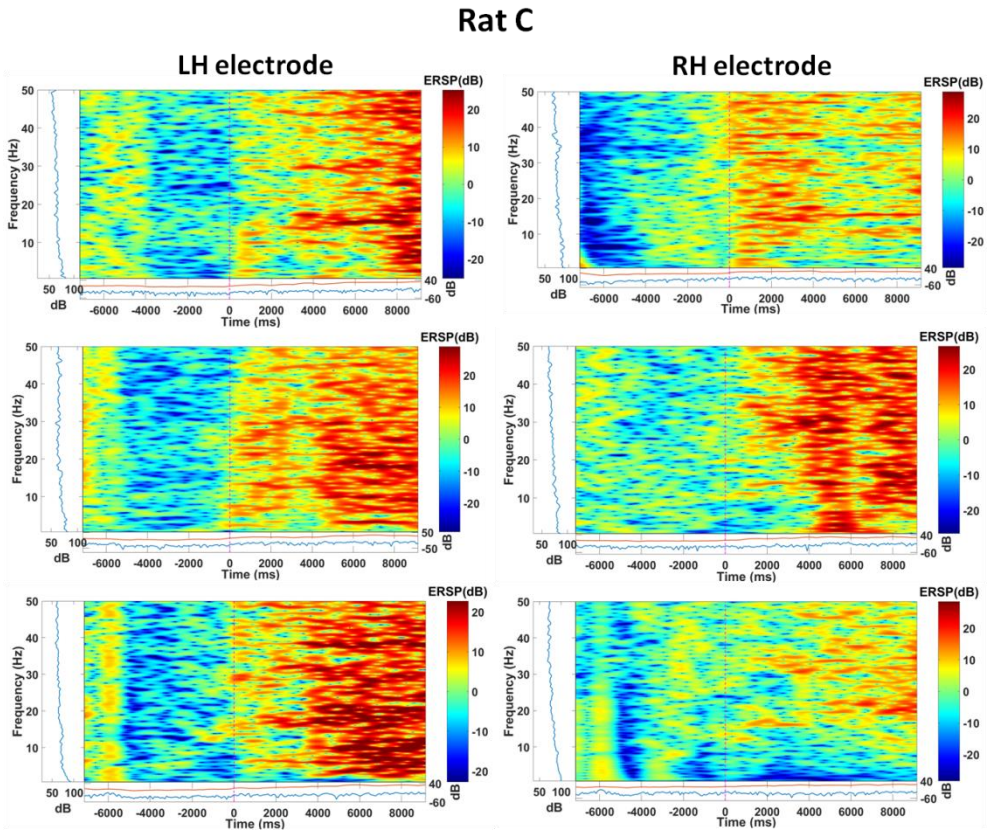

Figure 3. An example of the time frequency plots of the three 22 seconds peri-ictal segments for one rat, used from data recorded at the RH (left) and LH (right) sources. Time 0 indicates the seizure onset.

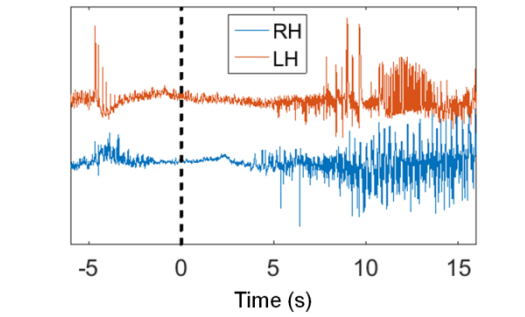

Figure 4. An example of peri-ictal activity from one rat as recorded in the lesioned (RH) and perilesional (LH) hippocampi

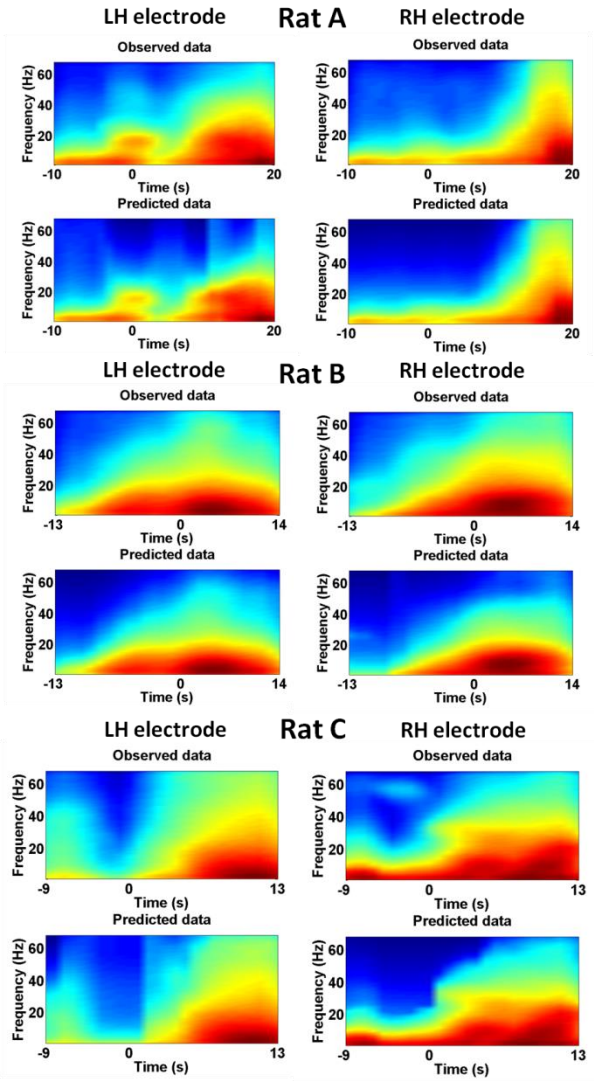

Figure 5. Smoothed and averaged time frequency representations of observed (upper panels) and predicted peri-ictal activity (lower panels) in the RH (left) and LH (right) sources, under the full model for each of the three rats. The electrographic seizure onset is at 0 seconds.

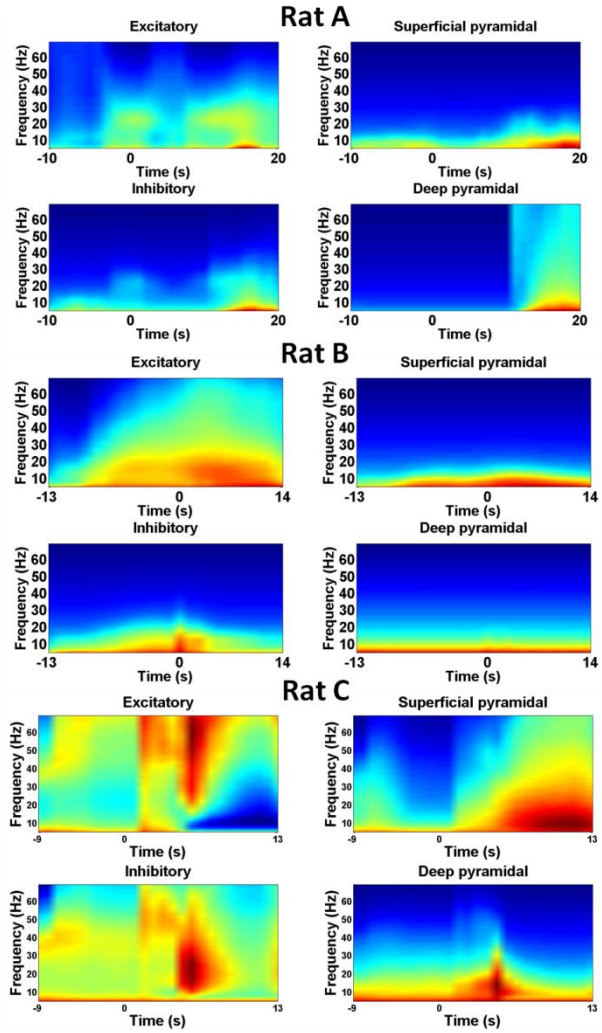

Figure 6. Time frequency representation of the modelled peri-ictal activity of the four subpopulations comprising the CMC model of the RH source for each of the 3 rats.

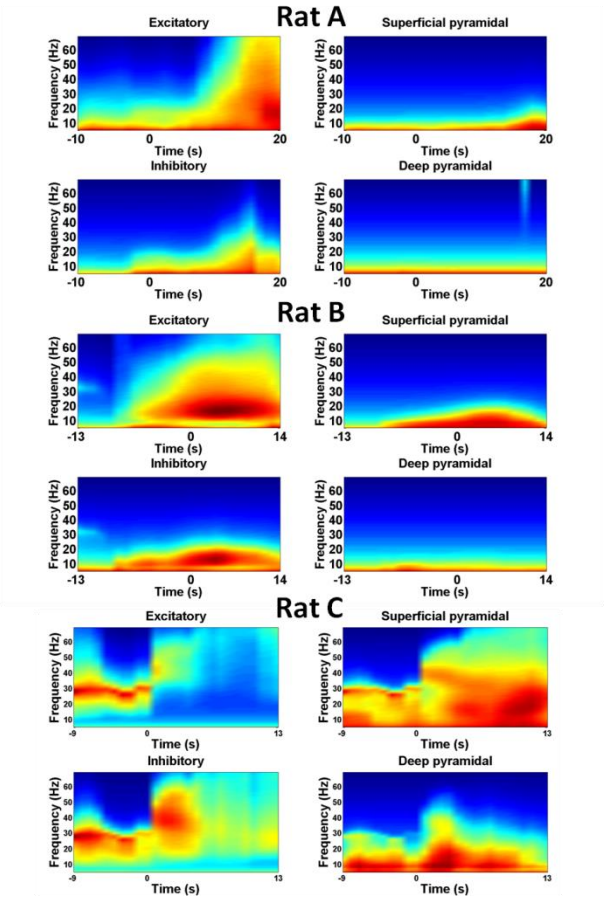

Figure 7. Time frequency representation of the modelled peri-ictal activity of the four subpopulations comprising the CMC model of the LH source for each of the 3 rats.

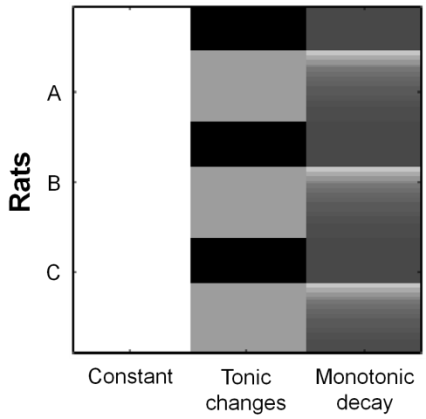

Figure 8. Second level design matrix

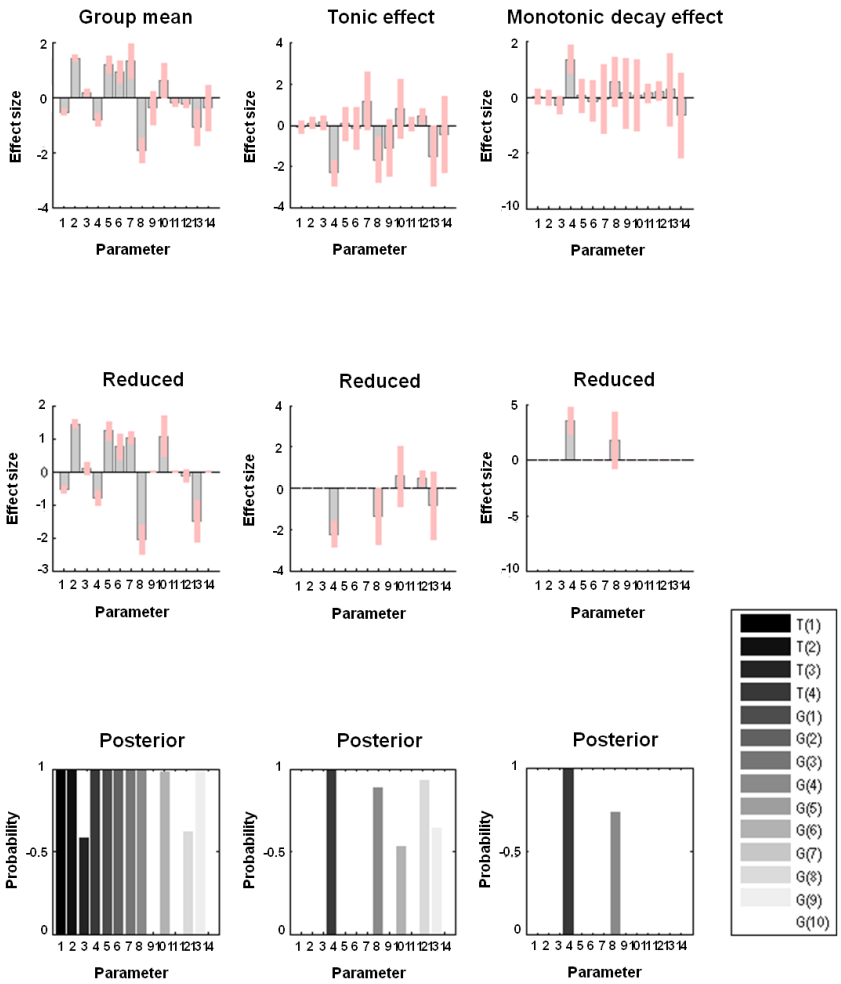

Figure 9. Results of Bayesian model comparison testing for changes in intrinsic connectivity parameters (RH lesional source). The left panel is showing the results for the group mean, while the middle and right panels, show the Bayesian model averages of the sustained increases in each parameter following seizure onset as well as the influence of two between-subjects covariates on each connection. The top row reports the posterior expectations (grey bars) and 90% Bayesian confidence intervals (pink bars) for each (second level) parameter before model reduction. Some of these parameters are eliminated following Bayesian model reduction, leaving the parameters in the middle row. The probability of models with and without these parameters is provided in the lower row. The results for the first covariate (tonic effect) show that we can be almost certain that connectivity parameters 4, 8, 10, 12 and 13 are necessary to explain seizure activity, as summarised by their spectral density. In particular, there appear to be profound reductions in parameters 4 and 8 that correspond to the synaptic time constant of the deep pyramidal cells and the self-inhibition of inhibitory interneurons (see Table 1). The results for the second covariate (exponential decay) show that we can be almost certain that connectivity parameters 4, 8 are necessary to explain seizure onset which are the same parameters they had a profound reduction for tonic covariate where now one can notice a profound increase.

This inference is based upon a second level (empirical Bayesian) model that allows for between epoch effects. The results shown here assume the same effects were expressed in all three rats. In other words, we averaged between epoch effects over subjects.

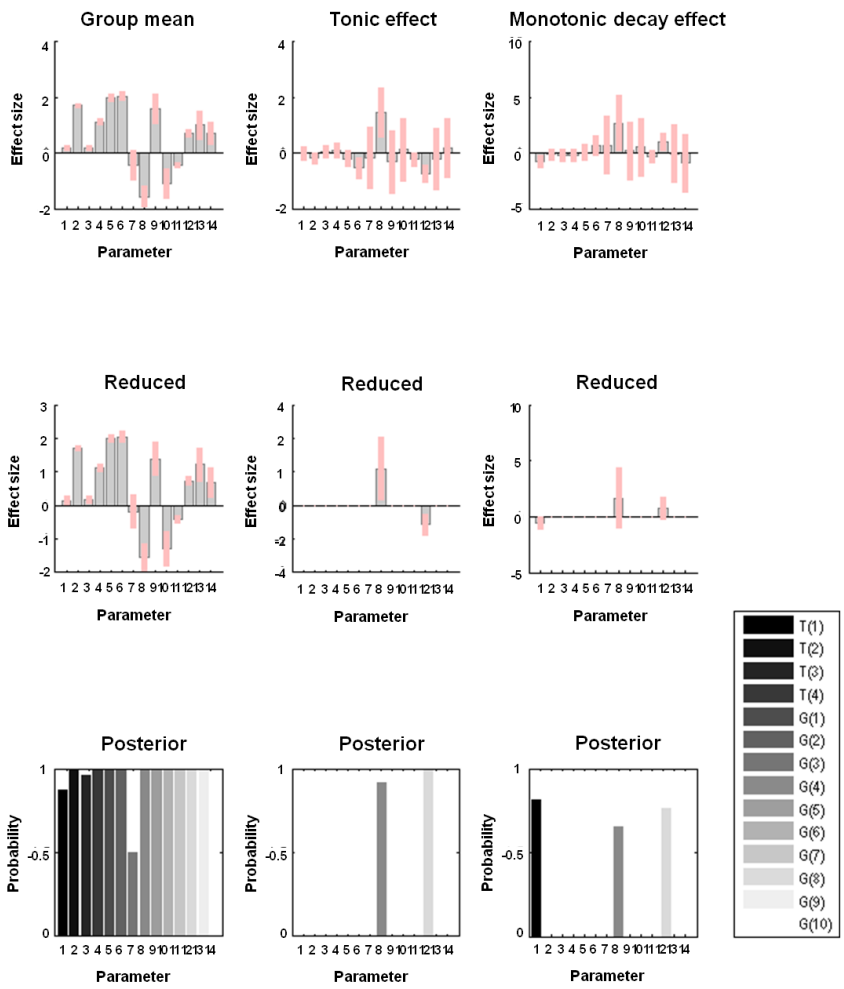

Figure 10. Results of Bayesian model comparison testing for changes in intrinsic connectivity parameters (LH source perilesional source). This figure uses the same format as the previous figure to report the Bayesian model averages of group means (left column) and sustained and transient changes (middle and right columns) following Bayesian model reduction. For the tonic changes parameters 8,12 (see Table 1) were sufficient to explain the seizure onset where for the exponential decay one extra parameter is added (first parameter of Table 1).

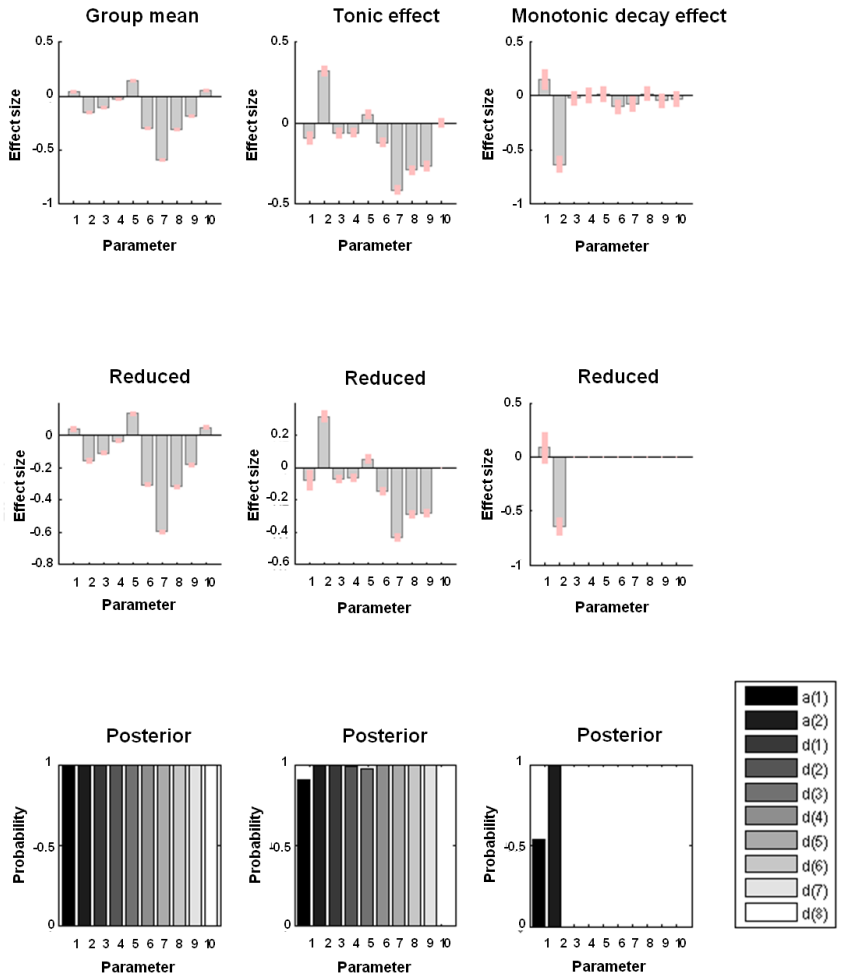

Figure 11. In this figure, the results relate to the parameters of endogenous activity (RH lesional source). The first two parameters pertain to the amplitude and experiment of scale-free fluctuations, while the remaining eight parameters encode a discrete cosine basis set over frequencies.

The key result for the first covariate (tonic changes) here is that the scale parameter of endogenous fluctuations increases markedly during seizure activity for the first covariate, suggesting a shift from higher frequencies to lower frequencies after seizure onset. The inverse effect is observed for the monotonic decay with a marked increase of the same scale parameter of endogenous fluctuations at the seizure onset.

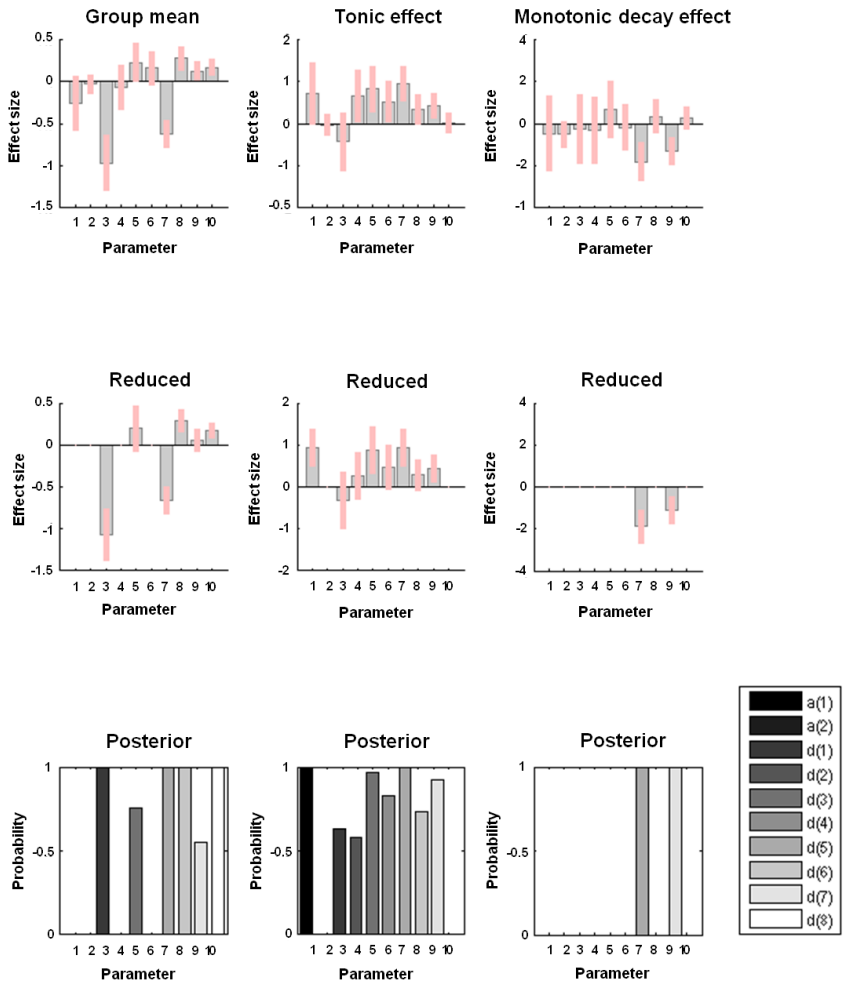

Figure 12. As in figure 11, the results relate to the parameters of endogenous activity but in the LH perilesional hippocampus. Here we see a similar pattern with the one of lesional hippocampus with almost all endogenous activity parameters needed to explain the seizure onset for the first covariate and only two for the second.